Diamond coatings on femtosecond-laser-textured stainless steel 316 surfaces for enhanced adherence

Zhipeng Wu, Wanting Sun, Aofei Mao, Qiuchi Zhu, Xin Chen, Xiang Zhang, Lanh Trinh, Nan Li, Xi Huang, Nada Kraiem, et al.

Diamond Coatings on Femtosecond-Laser-Textured Stainless Steel 316 Surfaces for Enhanced Adherence

Zhipeng Wu[a,#], Wanting Sun[a,#], Aofei Mao[a], Qiuchi Zhu[a], Xin Chen[b], Xiang Zhang[b], Lanh Trinh[b], Nan Li[a], Xi Huang[a], Nada Kraiem[a,c], Jean-François Silvain[a,c], Bai Cui[b], Yongfeng Lu[a,*]

[a] *Department of Electrical and Computer Engineering, University of Nebraska, Lincoln, NE 68588, USA.*

[b] *Department of Mechanical and Materials Engineering, University of Nebraska, Lincoln, NE 68588, USA.*

[c] *CNRS, Univ. Bordeaux, Bordeaux INP, ICMCB, UMR 5026 F-33608, Pessac, France.*

#Zhipeng Wu and Wanting Sun contributed equally to this work.

**Corresponding author. Email: ylu2@unl.edu*

Abstract: A challenge for directly coating diamond on metallic substrates is the large residual stress near their interfaces due to the large mismatch in the coefficients of thermal expansion (CTEs) that leads to cracking or delamination of the diamond coatings from the substrates. In this work, femtosecond (fs)-laser texturing was applied to fabricate various periodic microgrids on stainless steel (SS) 316 substrates for enhancing the adherence between the SS 316 substrates and the diamond coatings grown using the laser-assisted combustion flame chemical vapor deposition (CVD). Through adjusting the dimensions of the microgrids with different fs scanning parameters, the diamond coatings with a maximum thickness of 19 μm can be grown with quality factors up to 96% as analyzed by Raman spectroscopy. The corresponding large diamond crystals with an average grain size of 9 μm can be obtained on SS316 substrates by optimizing the fs-laser texturing process. The enhanced adherence between the SS 316 substrates and diamond coatings can be attributed to the stress relief and the improved mechanical bonding. The growth kinetics of the diamond coatings on fs-laser-textured SS 316 substrates were also revealed through the phase constitutions and morphology characteristics. This work is

anticipated to provide a new strategy and guidance for the growth of diamond coatings on metallic materials with strong adherence at the interfaces.

Keywords: Femtosecond-laser texturing; Laser-assisted combustion flame chemical vapor deposition; Growth kinetics of diamond coatings.

1. Introduction

Diamond is a unique material with excellent properties including high hardness, high thermal conductivity, chemical inertness, broad-spectrum optical transparency, and electrical insulating properties, which have all been extensively applied in the optical, mechanical, thermal and electronic domains [1-3]. In particular, chemically inert diamond coatings with high corrosion resistance can protect steel components from environmental erosion. Possible applications of diamond-coated steel substrates include and are not limited to cutting tools, bearings, and sensors in harsh environments. Diamond coatings on iron (Fe)-based substrates have attracted tremendous attention for applications under extreme conditions [4,5]. It has been demonstrated that the diamond coatings with high quality and large grains can be successfully deposited on the WC-Co substrates using the laser-assisted combustion flame chemical vapor deposition (CVD) method [6,7].

However, diamond coating on steel substrates using CVD method poses significant challenges. i) Carbon atoms have a high solubility and a high diffusion coefficient within the austenitic steel substrates leading to severe internal carburization of the steel substrate and generation of a Fe_3C layer [8,9]. Reactive transitional metals, such as Fe, cobalt (Co), and nickel (Ni), have strong catalytic effects on graphite formation [8,9]. Accordingly, the decomposition of metastable Fe_3C phase and the formation of a graphite layer on the surface of steel substrates are induced by catalytic graphitization. It has been reported that diamond coatings can grow on the graphite layer under a favorable gas phase for diamond formation [5,8]. Nevertheless, the graphite interlayer usually exhibits a weak interfacial bonding with the steel substrate, which causes the diamond coating to easily peel off from the steel substrate [10]. ii) Large residual internal stress derived from the large mismatch in CTEs between diamond and steel substrates [11] (mean CTEs of the polycrystalline CVD diamond and the austenite-ferrite transforming steel from 865 to 35 ℃: $\alpha_{diamond} \approx 3.5\times10^{-6}$ /K, $\alpha_{steel} \approx 10.7\times10^{-6}$ /K) occurs during diamond deposition, which leads to cracks and delamination of diamond coatings from steel substrates [5].

As shown in Fig. S1, the diamond coating deposited on the bare SS 316 substrate experienced breakage during the cooling process following a rapid removal of the SS 316 substrate from the oxygen-acetylene flame.

Numerous attempts have been made to improve the adherence between Fe-based substrates and diamond coatings. Recently, introduction of interlayers and surface modification have become the two most common methods to construct strong binding interfaces. For example, internal carburization can be significantly hindered by the presence of an interlayer. Thereby the catalytic graphitization effects are suppressed. In general, borides (FeB and Fe_2B [12]), carbides (SiC 14], CrC [15] and VC [16, 17]), and nitrides (CrN [18] and TiN [19]) are considered to be the most common interlayers for diffusion barriers. However, it is difficult for the reported interlayers to satisfy the requirements for compensating such large CTE mismatch between diamond and Fe-based substrates [20,21]. Therefore, surface modification can provide an effective alternative to alleviate the internal stress caused by the large CTE mismatch [6,11]. The inclination of the modified surface from the direction of the maximum compressive stress can change its distribution at the interfaces. The coatings can then be mechanically interlocked to the substrates, leading to higher adhesion strength [20]. In addition, the interfacial area is also enlarged by the surface roughness to provide numerous nucleation positions. The mechanical anchoring between the coatings and substrates is promoted [23]. Previous studies demonstrated that surface modification can play important roles in improving the adhesion strength between diamond coatings and substrates, such as Mo [24], WC [6], Si_3N_4 [25]. It was also found that surface modification by sandblasting was beneficial to improve the adherence between stainless steel (SS) 304 substrates and diamond coatings, which was ascribed to the occurrence of phase transformation and rough surfaces [26]. However, apart from residual particles, the stochasticity of the blasted surfaces is high, which limits their reproducibility and modification options [27]. Recently, laser surface texturing has been developed as a novel, efficient, and economical technique to increase the surface roughness of substrates and the contact areas between substrates and coatings. For example, plasma-assisted nanosecond (ns) laser machining was used to enhance the adhesion of TiAlN coatings on WC/Co substrates, which exhibit a higher critical load than that of the TiAlN coatings on polished samples during the scratch test [23]. Laser texturing was also found effective in enhancing adhesion of plasma-sprayed Ni-5Al coatings on the 2017 Al alloy [28]. Additionally, finite element analyses were conducted to investigate the

stress distributions in diamond and diamond-like carbon coatings on the textured steel substrates [27, 29]. It shows that the stress distribution in the coatings on the textured surfaces is significantly changed as compared to that of the smooth surfaces. For coatings on the laser-textured surfaces, the tensile and compressive stresses appear near the peaks and the valleys, respectively. In contrast, the compressive stress is distributed in the coatings on smooth surfaces. Therefore, to mitigate the effect of the large CTE difference between diamond coatings and metallic materials, laser texturing provides an efficient and reliable way to modify the surface, redistribute the stress and improve the mechanical bonding.

In this study, various periodic microgrid structures were fabricated on SS 316 substrates using a femtosecond (fs) laser. The microgrid structures showed positive effects on the preparation of adherent diamond coatings on SS 316 substrates, which can be attributed to the stress relief and the improved mechanical bonding. The growth kinetics of diamond coatings were also revealed by the phase constitutions and morphology observations during different diamond deposition times.

2. Experimental sections

2.1. Substrate Pretreatments

Commercial SS 316 plates (OnlineMetals.com) with chemical compositions of 82 wt.% Fe, 18 wt.% Cr, 14 wt.% of Ni, 3 wt.% of Mo, 2 wt.% of Mn, and 0.08wt. % of C were used as substrates. The plates were cut into $10\times10\times1$ mm^3, followed by ultrasonically cleaning in acetone for 10 min.

The laser texturing was performed on the SS 316 substrates using a fs laser (Amplitude Inc, Tangor) in the ambient air. Various periodic microgrids were fabricated by adjusting the laser scanning passes. Fig. 1a illustrates the schematic of the fs-laser texturing setup. The periodic microgrid patterns were achieved by scanning the laser spot in two perpendicular directions. The laser beam with a wavelength of 1030 nm was controlled by a galvanometer scanner (SCANLAB GmbH). The fs laser was focused on the SS 316 substrates with a spot diameter of 30 μm and scanned at a speed of 1 m/s with a 408-fs pulse duration and 330 kHz frequency for 25, 45 and 75 scanning passes, respectively. The laser power and pitch distance used in the laser texturing were 14 W and 60 μm, respectively.

2.2. Diamond Deposition

After the fs-laser texturing, the substrates with microgrids were ultrasonically seeded in a suspension of diamond slurry, which were mixed by 0.1 g nanodiamond (particle size: <10 nm, purity: 97.0+%, TCI America™) and 30 mL 200 proof ethyl alcohol (≥99.5%, Sigma-Aldrich). As shown in Fig. 1b, the diamond coatings were deposited using a laser-assisted combustion flame CVD system in open air [6,7]. The gas precursor was a mixture of acetylene (C_2H_2, 99.999%), ethylene (C_2H_4, 99.6%), and oxygen (O_2, 99.996%) with a flow rate ratio of 910:400:1200 standard cubic centimeter per minute (sccm), respectively. In this system, a wavelength-tunable continuous-wave CO_2 laser (XL1000, PRC Laser Corporation) was used in the combustion flame system. The average laser power was set at 250 W and the wavelength was set at 10.532 μm to match the CH_2-wagging vibrational mode of the ethylene molecules [30, 31] to promote the diamond growth. A textured substrate was placed under the torch using a motorized X-Y-Z stage. The substrate temperature was measured by an infrared pyrometer (OS3752, Omega Engineering, Inc.) and maintained at around 720 ℃ during diamond deposition using a water-cooling system. The deposition time and microgrid depths for different samples are listed in Table 1.

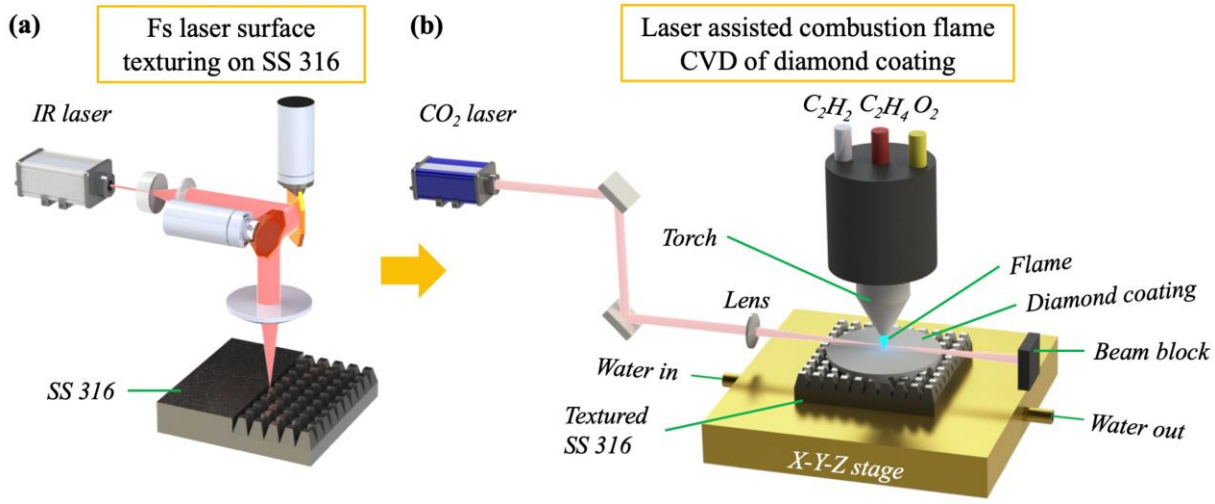

Fig. 1. Schematics of (a) SS 316 surface texturing using a fs-laser and (b) CO_2 laser-assisted combustion flame CVD of diamond coatings on the textured SS 316 substrates.

Table 1. Parameters of microgrid depths and deposition periods for different sample.

Sample Name	Microgrid Depth (μm)	Deposition Period (min)
SS0-D5	N/A	5
SS40-D0	40	N/A
SS10-D30	10	30
SS25-D30	25	30
SS40-D5	40	5
SS40-D10	40	10
SS40-D20	40	20
SS40-D30	40	30

2.3. Characterizations

Characterization of the surface morphology of the diamond coatings were conducted using an FEI Quanta 200 Environmental scanning electron microscope (SEM). To determine the thickness of the diamond coatings deposited, the as-prepared samples were covered with a thick layer (~500 μm) of PELCO conductive silver paint (Ted Pella, Inc.) before cutting using electrical discharge machining. The cross-sectional planes were then examined by SEM. The chemical compositions of the interface between the diamond coating and SS 316 substrate were detected using energy dispersive spectrometry (EDS, Octane Super, EDAX). The phase constitutions of the initial and diamond-coated SS 316 substrates were investigated with X-ray diffraction (XRD) using a PANalytical Empyrean X-ray diffractometer (PANalytical, Westborough, MA) with a 1.4 kW copper Kα source (λ = 1.54187 Å) and a step size of 0.02° for 2θ. The quality of the diamond coating and residual stress were evaluated using a Raman spectrometer (inVia, Renishaw). A 514.5 nm argon-ion laser with a power of 50 mW was used as the exciting source for the Raman spectrometer. The laser beam was focused to a spot diameter of approximately 5 μm.

3. Results and discussions

3.1. Substrate morphologies after fs-laser texturing

Fig. 2 shows surface morphologies of the fs-laser textured SS 316 substrates processed by different laser scanning passes. Microgrids with trenches of 10, 25, and 40 μm can be fabricated by 25, 45 and 75 scanning passes, respectively. When the laser scanning pass is increased, the depth of the microgrids becomes larger, which is derived from the increase in the material ablation due to the increased delivered energy. It should be noted that the grid pitch is maintained at about 60 μm.

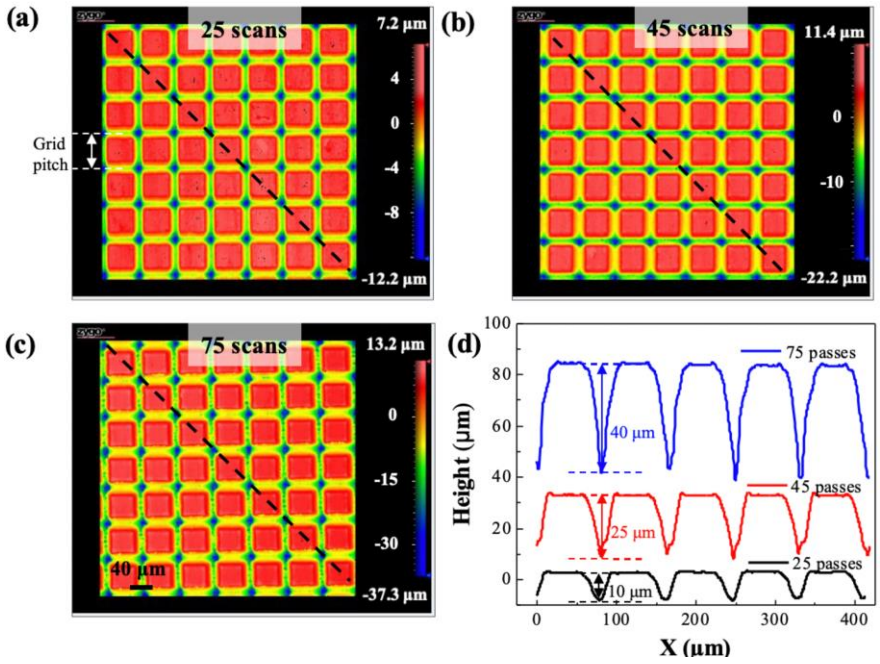

Fig. 2. Zygo mappings of the fs-laser textured SS 316 substrates with: (a)-(c) 25, 45 and 75 scanning passes. (d) diagonal profiles obtained from (a)-(c) as marked by the dashed lines.

3.2. Microstructural analyses of diamond coatings

The fs-laser textured SS 316 substrates above were used for diamond deposition using the CO_2 laser-assisted CVD method. The deposited diamond coating forms a circular area with its center positioned beneath the inner flame tip. The grain sizes consistently remain above 85% of the maximum within a diameter of 3 mm and decrease towards the edges. Fig. 3a shows the microstructures of the diamond coating on a bare SS 316 substrate after 5 min of deposition. A diamond coating with a large area can be achieved, but such coating is easily broken-up and

peeled off from the bare SS 316 substrate, indicating that the diamond coating is not stable. The residual stress near the interface produced by the large CTE difference between the diamond coating and the SS 316 substrate leads to a broken-up diamond coating [5]. Fig. 3b shows the SEM micrograph of the fs-laser textured SS 316 substrate. The top surface remained flat after fs-laser texturing. Fig. 3c, d and h present diamond coatings on SS 316 substrates with microgrid depths of 10, 25 and 40 μm, respectively. The deposition time was maintained constantly at 30 min. As compared to the diamond deposited on the bare SS 316 substrate, the diamond coatings are firmly attached to the fs-laser textured SS 316 substrates. It suggests that the adherence of diamond coating can be remarkably improved by the introduction of microgrids on SS316 substrates. Additionally, when the depth of the microgrids was increased from 10 to 40 μm, the average grain size of the diamond coatings increased from 1.5 to 9 μm, indicating that the deposition process can be promoted by the increase in the microgrid depth. The reason for the enhancement of growth can be attributed to the increased local temperature resulting from the promoted heat transfer by the expanded surface area [32,33].

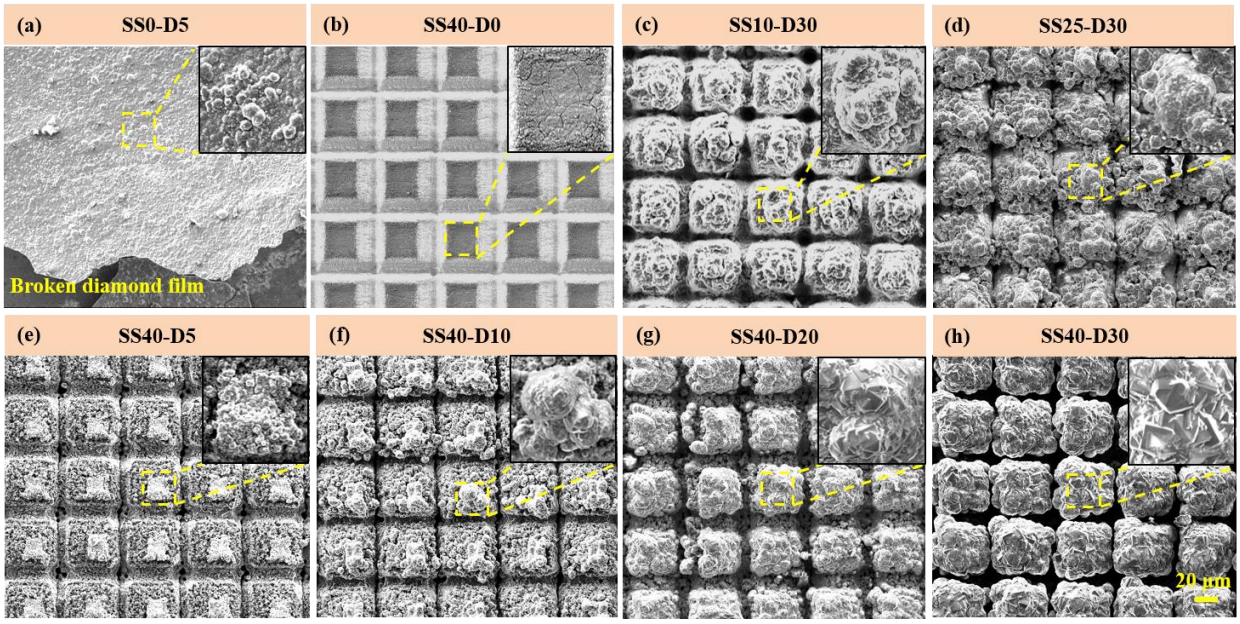

Fig. 3. SEM micrographs of (a) a diamond coating deposited for 5 min on the SS 316 substrate without fs-laser treatment, (b) a fs-laser textured SS 316 substrate with a microgrid depth of 40 μm, (c),(d) diamond coatings deposited on the fs-laser textured SS 316 substrates for 30 min with the microgrid depths of 10 and 25 μm, respectively; (e)-(h) diamond coatings deposited on the fs-laser textured SS 316 substrates with microgrid depths of 40 μm for 5, 10, 20 and 30 min, respectively.

To reveal the growth dynamics of the diamond coatings, the deposition time was varied from 5 to 30 min with the microgrid depth maintained at 40 μm. As shown in Fig. 3e, for the deposition time of 5 min, diamond coatings with an average grain size of 1 μm were obtained in a rectangular shape on the top surface of the microgrids, indicating that the diamond growth rate on the top surface is more rapid than that of the surroundings. The round and drop-shaped structures near the grid edges are inferred to be a consequence of metal dusting, including graphite formation and decomposition of Fe_3C [34]. With the increase in the deposition time, the grains of the diamond coatings were significantly enlarged when the coating area were expanded. It can be observed from Fig. 3h that, after a deposition time of 30 min, the entire top surface of the microgrids were covered with the diamond coating which had an average grain size of 9 μm.

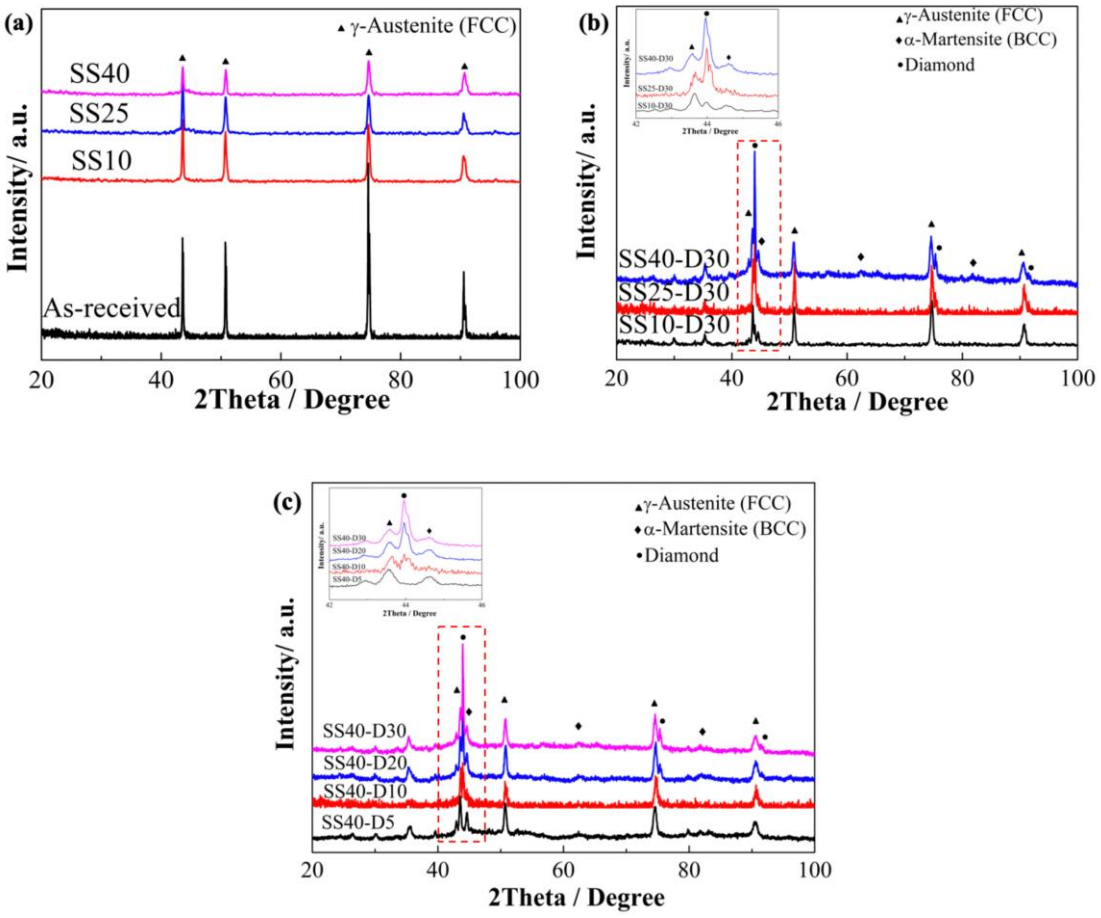

Fig. 4. XRD patterns of the SS 316 substrates (a) before and after fs-laser texturing with microgrid depths of 10, 25 and 40 μm, respectively; (b) with diamond coatings on the 10, 25 and 40 μm microgrids, respectively; (c) with diamond coatings on the 40 μm microgrid for deposition periods of 5, 10, 20 and 30 min, respectively.

Fig. 4a presents the XRD patterns of the SS 316 substrates before and after fs-laser texturing. It is apparent that the initial as-received SS 316 is mainly composed of γ-austenite phase. By comparison, there is no significant change in the phase constitutions of SS316 substrates after the fs-laser texturing. It can be explained by the fact that fs-laser texturing belongs to a cold processing method due to the ultrashort laser pulses. Fig. 4b shows the XRD patterns of the diamond-coated SS 316 substrates with different microgrid depths. After the deposition of diamond coating, the austenite phase of the SS 316 substrates remained. Besides, the diffraction peaks located at 2θ of 43.9°, 75.1°and 91.5° can be detected, which can be attributed to the characteristic lattice planes of (111), (220), (311) of diamond [35]. The (111) peak intensity of diamond increases with the increase in the microgrid depth, further indicating that an increase in the relative diamond ratio can be facilitated by the introduction of the microgrids on the SS316 substrates. Fig. 4c shows the XRD patterns of the diamond-coated SS 316 substrates with the microgrid depth of 40 μm for various deposition periods of 5, 10, 20 and 30 min, respectively. The intensities of the diamond characteristic diffraction peaks are enhanced when the deposition time is gradually increased from 5 and 30 min. The quality of the deposited diamond increases with microgrid depth and deposition time. It should be also noted that the phase transformation from austenite to martensite can be detected, resulting from the metal dusting [34] and thermal effect induced by the diamond deposition at the temperature of 720 ℃.

To further analyze the morphology evolution and chemical compositions near the interface between the diamond coatings and the SS 316 substrates, the cross-sections of the diamond-coated SS 316 substrates with the microgrid depths of 10, 25 and 40 μm are presented in Fig. 5. As shown in Fig. 5b, e and h, with the increase in the microgrid depth, the thickness of the diamond coatings is also increased. When the microgrid depth reaches 40 μm, a diamond coating with a thickness of 19 μm can be obtained. It further verifies that diamond deposition is enhanced by the increased depth of the microgrids. It should be noticed that the coating thickness was maximized at the center of the circular coated area and decreased towards the margins of the area. The formation of diamond coating is also confirmed by the corresponding EDS results. An interlayer containing both C and Fe elements can be detected between the diamond coatings and the steel substrates. As reported, the steel substrate is presumably carbonized and a carbide interlayer is formed at the initial stage, followed by the deposition of the iron carbides into graphite and iron [8,9,34].

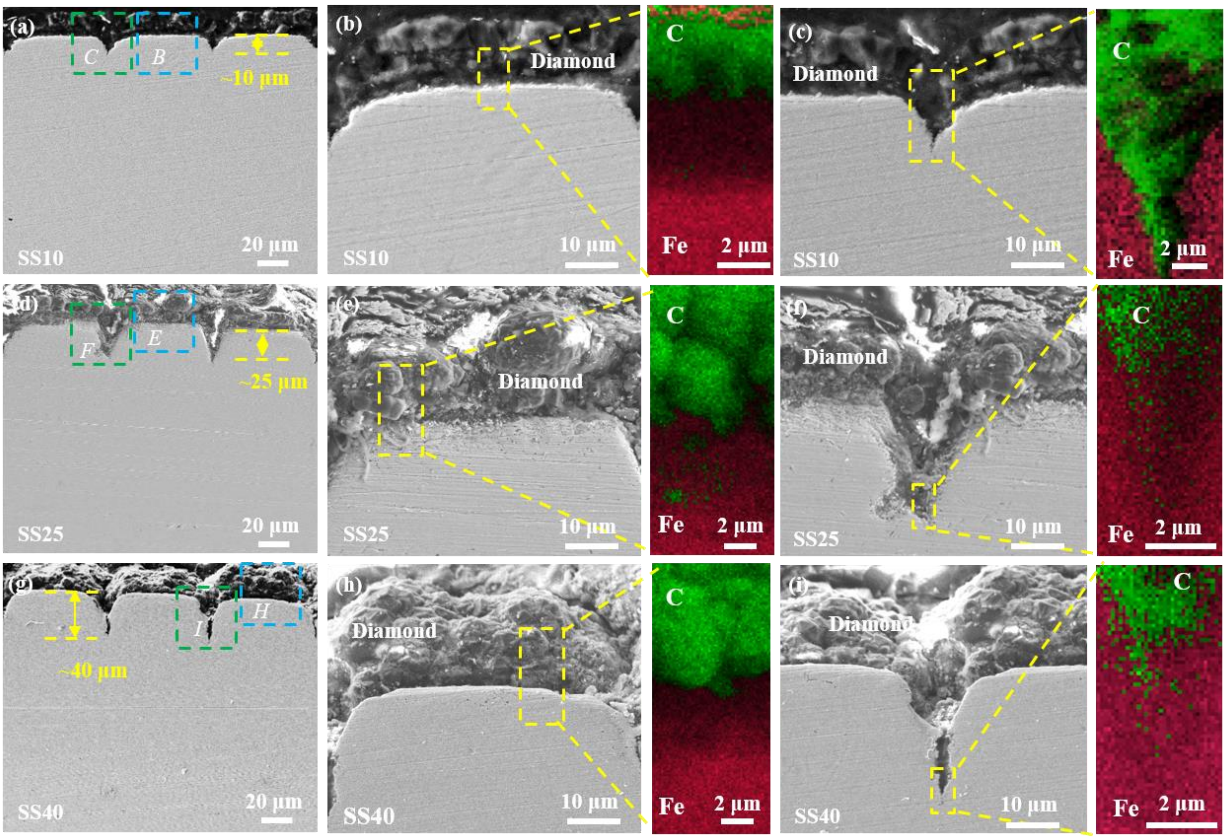

Fig. 5. Cross-sectional SEM micrographs of diamond-coated SS 316 substrates (a) with a microgrid depth of 10 μm, (b) at the center of the 10 μm microgrid, (c) at the valley of the 10 μm microgrid, (d) with a microgrid depth of 25 μm, (e) at the center of the 25 μm microgrid, (f) at the valley of the 25 μm microgrid, (g) with a microgrid depth of 40 μm, (h) at the center of the 40 μm microgrid, and (i) at the valley of the 40 μm microgrid.

3.3. Quality and residual stress analyses of diamond coatings

The quality of diamond coatings on the top surface can be evaluated by Raman spectra as shown in Fig. 6. It reached the maximum at the center of the circular coated area and degraded towards the margins of the area. Generally, the sharp peak located around 1332 cm^{-1} can be assigned to the sp^3 hybridized crystalline diamond. Besides, the D- and G-bands at ~1350 and ~1580 cm^{-1} can be assigned to the disordered and sp^2 hybridized crystalline graphite in the coatings, respectively. The broadband centered between 1500 and 1550 cm^{-1} is related to the formation of amorphous carbon in the diamond coatings [36]. As shown in Fig. 6a, with the increase in the deposition time, the intensity of the diamond peak gradually becomes higher, whereas the intensities of the D and G bands become lower, indicating that a purer diamond

phase with a higher diamond quality can be achieved. Fig. 6b presents the Raman spectra of the diamond coatings deposited on the SS 316 substrates with microgrids of various depths. When the diamond deposition time is fixed at 30 min, the diamond peak become sharper with the increase in the microgrid depth, while the intensities of the D and G bands are gradually reduced. Based on the Raman spectra, the quality factor can be used to evaluate diamond coatings using the following equation [37]:

$$Q_i = I_{diamond}/(I_{diamond}+I_{a\text{-}carbon}/233), \quad (1)$$

where $I_{diamond}$ and $I_{a\text{-}carbon}$ are the integrated intensities of the diamond peak and the sum of the integrated intensities of the nondiamond carbon bands, respectively.

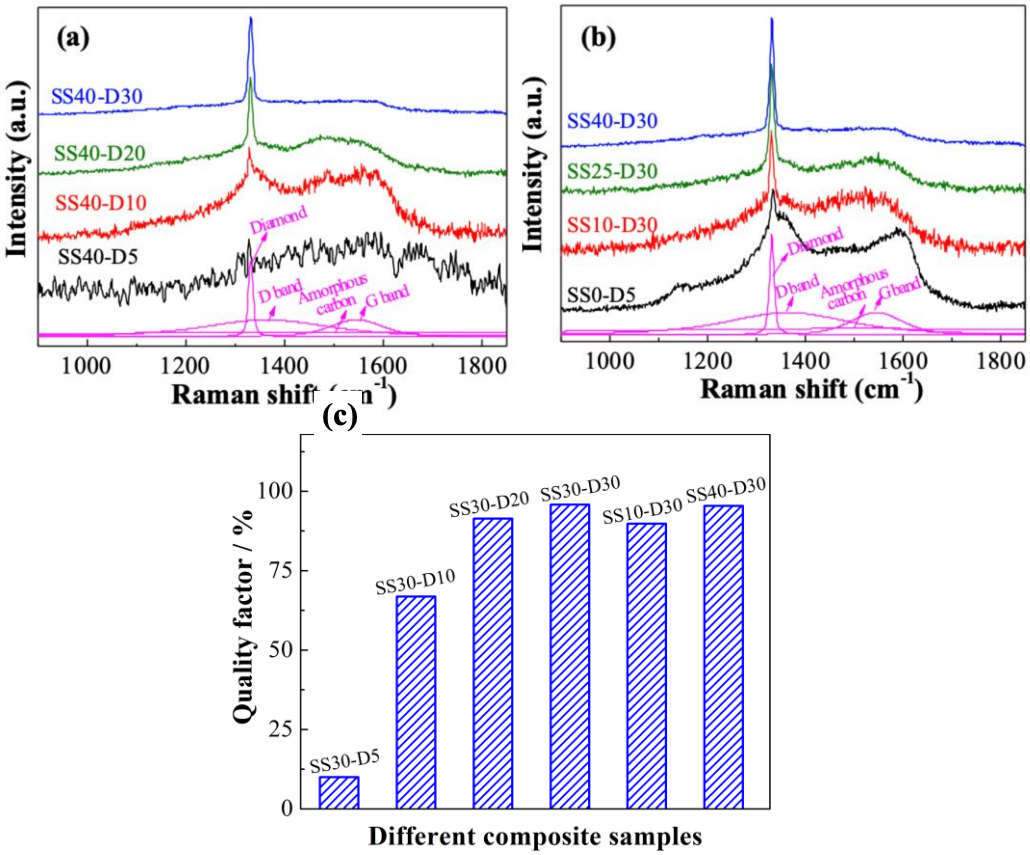

Fig. 6. Raman spectra of the diamond coatings deposited on the fs-laser textured SS 316 substrates (a) with a microgrid depth of 40 μm after deposition times from 5 to 30 min, (b) with the microgrid depths of 0, 10, 25 and 40 μm after 30 min of deposition, (c) the diamond quality factors calculated based on the Raman spectra.

As can be seen from Fig. 6c, during the deposition, the coatings with a mixture of diamond and graphite can be generated on the fs-laser textured SS 316 substrates. After 10 min of

deposition, the graphite content in the diamond coating is relatively high because the Fe element in the SS 316 could catalyze the formation of graphite [9]. With the increase in the deposition time, the SS 316 substrate is covered with the diamond coating and the catalysis effect of Fe is weaker, leading to the formation of a purer diamond coating. The quality factor of diamond is increased from 10% to 96% with increasing deposition times from 5 to 30 min. Furthermore, when the microgrid depth on the SS 316 substrates is increased from 10 to 40 μm, the quality factor of the diamond coatings increases from 89% to 96%, indicating that higher diamond quality can be obtained by larger microgrid depth. The enhanced growth of diamonds is inferred to be a consequence of the increased local temperature due to the promoted heat transfer by the expanded surface area [32,33].

Based on the positions of the diamond peaks, the residual stress in the diamond coatings on the top surface can be estimated. The residual stress is inversely proportional to the Raman peak shift [38-40]:

$$\sigma = -0.567*(\nu_m-\nu_0), \quad (2)$$

where ν_m and ν_0 are the Raman peak positions of the measured and pure diamond, respectively. To obtain the Raman positions of the diamond peaks, Fig. 7a and c show the Raman spectra near 1332 cm^{-1} with variation in the deposition time and the microgrid depth, respectively. Fig. 7b summarizes the calculated residual stresses in Fig. 7a against deposition time while the depth of microgrids was maintained as 40 μm. When the deposition time is increased from 10 to 30 min, the residual stress decreases from 1.9 to 0.46 GPa, demonstrating that a stronger adhesion can be produced between the diamond coating and SS 316 substrate. Fig. 7d, summarized from Fig. 7c, shows the residual stress variation against microgrid depth after 30 min of deposition. The diamond coating deposited on bare SS 316 substrate for 5 min exhibits a negative residual stress, indicating a compressive stress in the diamond coating. Due to the CTE of SS 316 (10.7×10^{-6}/K) being larger than that of diamond (3.5×10^{-6}/K), the steel substrate is subjected to more contraction than that of the diamond coating during the cooling process, which leads to the generation of compressive stress in the diamond coatings [26]. In contrast, the positive residual stress of the diamond coating on the fs-laser textured SS 316 substrate represents a tensile stress [27,29], which decreases from 1.2 to 0.46 GPa while the depth of the microgrids is increased from 10 to 40 μm, indicating that a stronger adhesion can be obtained between the diamond

coating and the substrate. The tensile stress is assumed to result from the bending of the diamond coatings over the shrinking substrates [11].

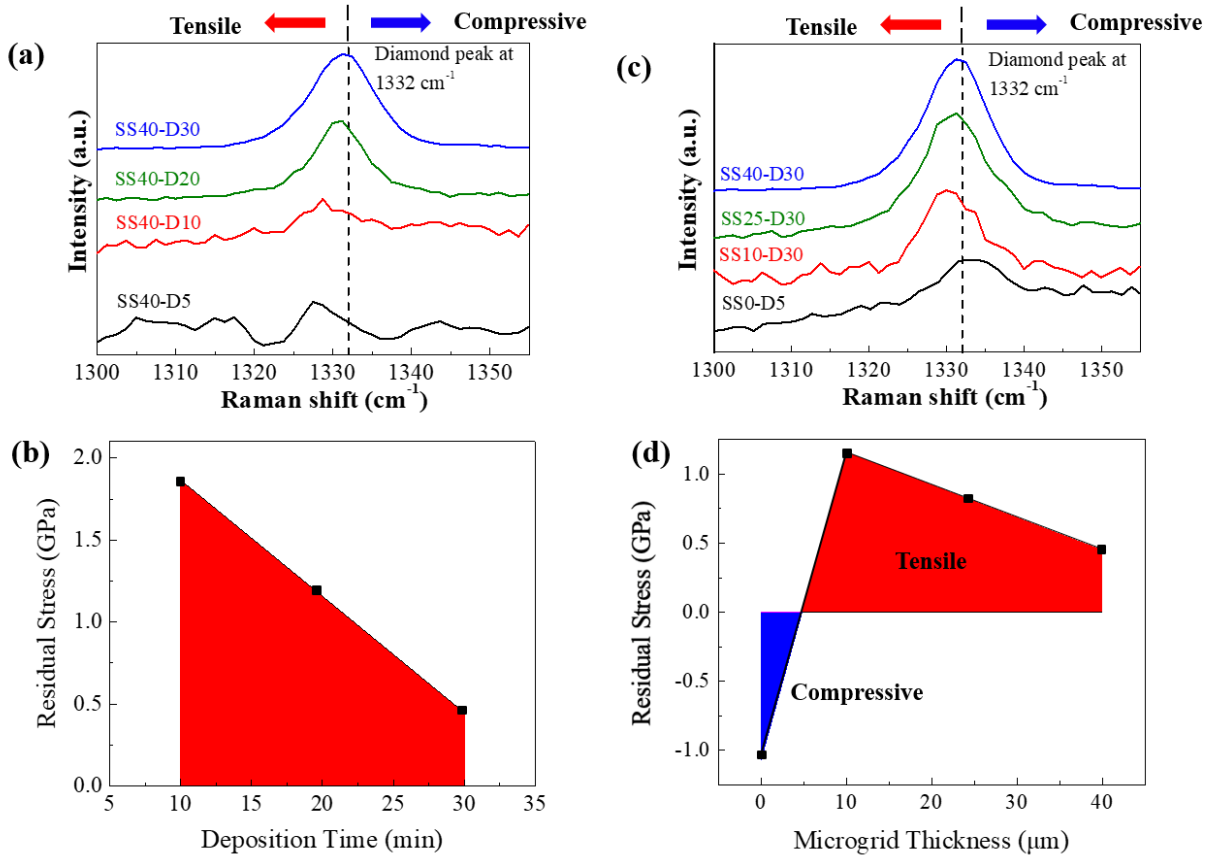

Fig. 7. Raman spectra near 1332 cm^{-1} and calculated residual stress of the diamond coatings deposited on the fs-laser textured SS 316 substrates (a), (b) after deposition from 5 to 30 min with the microgrid depth of 40 μm; (c), (d) with the microgrid depths of 10, 25, and 40 μm after 30 min deposition.

4. Conclusions

In this work, a fs-laser texturing method was developed to fabricate various periodic microgrids on SS 316 substrates for improving the adherence between SS 316 substrates and diamond coatings deposited through laser-assisted combustion flame CVD. The main conclusions can be drawn as follows:

(1) Diamond grain size, coating thickness, and diamond quality are enhanced with the increase in the microgrid depth. When the microgrid depth reaches ~40 μm, diamond coatings with a thickness of 19 μm and a quality factor of 96% were achieved.

(2) Compared to the bare SS 316 substrates, the microgrids fabricated by fs-laser texturing can promote the formation of firm diamond coatings. The stress relief effect and the increased

mechanical bonding induced by fs-laser texturing are responsible for the improved adhesion between the diamond coatings and SS 316 substrates. The residual stress in diamond coatings on the top surface can be transitioned from compressive to tensile. Meanwhile, the stress decreases with the increase in the microgrid depth on the SS 316 substrates.

(3) The growth dynamics of the diamond coatings on the fs-laser textured SS 316 substrates has been revealed. At the initial deposition stage, a layer containing both Fe and C is formed on the SS 316 substrates due to internal carburation. However, the catalytic graphitization effects of Fe, Co and Ni result in the decomposition of the intermediate layer, followed by graphite deposition. When increasing the deposition time under a diamond favorable gas phase, the graphite interlayer will be covered with the deposited diamond, and eventually, diamond coatings with a high-quality factor of 96% can be achieved.

Prime novelty statement

Fs laser texturing is capable of improving the adherence between diamond coatings and SS 316 substrates due to stress relief and improved mechanical bonding. Growth kinetic and effects of the texturing depth are systematically investigated.

Acknowledgements

This study was supported by the Nebraska Center for Energy Sciences Research (NCESR). The study was performed in part in the Nebraska Nanoscale Facility: National Nanotechnology Coordinated Infrastructure and the Nebraska Center for Materials and Nanoscience, which are supported by the National Science Foundation under Award ECCS: 1542182, and the Nebraska Research Initiative. The authors would like to thank Leo Lu for the assistance in the preparation of the manuscript.

Abbreviations

Fs, femtosecond; CVD, chemical vapor deposition; CTE, coefficient of thermal expansion; SS, stainless steel; ns, nanosecond; SEM, scanning electron microscopy; EDS, energy dispersive spectrometry; XRD, X-ray diffraction.

References

[1] M. Liao, Progress in semiconductor diamond photodetectors and MEMS sensors, Functional Diamond. 1 (2021) 29–46. https://doi.org/10.1080/26941112.2021.1877019.

[2] S. Pezzagna, J. Meijer, Quantum computer based on color centers in diamond, Applied Physics Reviews. 8 (2021) 011308. https://doi.org/10.1063/5.0007444.

[3] L. Sang, Diamond as the heat spreader for the thermal dissipation of GaN-based electronic devices, Functional Diamond. 1 (2021) 174–188. https://doi.org/10.1080/26941112.2021.1980356.

[4] X. Li, F. Xia, C. Wang, C. Chen, M. Jiang, J. Pan, S. Lu, A.A. Khomich, I. Vlasov, X. Hu, Deposition of an adherent diamond film on stainless steel using Cr/CrAlN as an interlayer, Surface and Coatings Technology. 449 (2022) 128960. https://doi.org/10.1016/j.surfcoat.2022.128960.

[5] X. Li, L. He, Y. Li, Q. Yang, Diamond Deposition on Iron and Steel Substrates: A Review, Micromachines. 11 (2020) 719. https://doi.org/10.3390/mi11080719.

[6] A. Veillère, T. Guillemet, Z.Q. Xie, C.A. Zuhlke, D.R. Alexander, J.-F. Silvain, J.-M. Heintz, N. Chandra, Y.F. Lu, Influence of WC-Co Substrate Pretreatment on Diamond Film Deposition by Laser-Assisted Combustion Synthesis, ACS Appl. Mater. Interfaces. 3 (2011) 1134–1139. https://doi.org/10.1021/am101271b.

[7] L.-S. Fan, L. Constantin, D. Li, L. Liu, K. Keramatnejad, C. Azina, X. Huang, H.R. Golgir, Y. Lu, Z. Ahmadi, F. Wang, J. Shield, B. Cui, J.-F. Silvain, Y.-F. Lu, Ultraviolet laser photolysis of hydrocarbons for nondiamond carbon suppression in chemical vapor deposition of diamond films, Light Sci Appl. 7 (2018) 17177–17177. https://doi.org/10.1038/lsa.2017.177.

[8] X.J. Li, L.L. He, Y.S. Li, Q. Yang, Catalytic graphite mechanism during CVD diamond film on iron and cobalt alloys in CH4-H2 atmospheres, Surface and Coatings Technology. 360 (2019) 20–28. https://doi.org/10.1016/j.surfcoat.2018.12.120.

[9] X. Sun, H.T. Ma, L.Z. Yang, M. Sanchez-Pasten, D. Craig Penner, Y.S. Li, Q. Yang, Metal dusting, carburization and diamond deposition on Fe–Cr alloys in CH4–H2 plasma

atmospheres, Corrosion Science. 98 (2015) 619–625. https://doi.org/10.1016/j.corsci.2015.06.001.

[10] X.J. Li, L.L. He, Y.S. Li, Q. Yang, A. Hirose, Direct Coating Adherent Diamond Films on Fe-Based Alloy Substrate: The Roles of Al, Cr in Enhancing Interfacial Adhesion and Promoting Diamond Growth, ACS Appl. Mater. Interfaces. 5 (2013) 7370–7378. https://doi.org/10.1021/am401709j.

[11] M. Göltz, T. Helmreich, R. Börner, T. Kupfer, A. Schubert, S. Rosiwal, Spatial distribution of thermally induced residual stresses in HF-CVD diamond coatings on microstructured steel surfaces, Diamond and Related Materials. 136 (2023) 109931. https://doi.org/10.1016/j.diamond.2023.109931.

[12] J.G. Buijnsters, P. Shankar, P. Gopalakrishnan, W.J.P. van Enckevort, J.J. Schermer, S.S. Ramakrishnan, J.J. ter Meulen, Diffusion-modified boride interlayers for chemical vapour deposition of low-residual-stress diamond films on steel substrates, Thin Solid Films. 426 (2003) 85–93. https://doi.org/10.1016/S0040-6090(03)00013-0.

[13] A. Contin, K.A. Alves, R.A. Campos, G. de Vasconcelos, D.D. Damm, V.J. Trava-Airoldi, E.J. Corat, Diamond Films on Stainless Steel Substrates with an Interlayer Applied by Laser Cladding, Mat. Res. 20 (2017) 543–548. https://doi.org/10.1590/1980-5373-MR-2016-0346.

[14] A. Contin, G. de Vasconcelos, D.M. Barquete, R.A. Campos, V.J. Trava-Airoldi, E.J. Corat, Laser cladding of SiC multilayers for diamond deposition on steel substrates, Diamond and Related Materials. 65 (2016) 105–114. https://doi.org/10.1016/j.diamond.2016.02.007.

[15] C. Bareiβ, M. Perle, S.M. Rosiwal, R.F. Singer, Diamond coating of steel at high temperatures in hot filament chemical vapour deposition (HFCVD) employing chromium interlayers, Diamond and Related Materials. 15 (2006) 754–760. https://doi.org/10.1016/j.diamond.2005.10.053.

[16] R.L. Martins, D.D. Damm, R.M. Volu, R.A. Pinheiro, F.M. Rosa, V.J. Trava-Airoldi, G. de Vasconcelos, D.M. Barquete, E.J. Corat, Laser cladding of vanadium carbide interlayer for CVD diamond growth on steel substrate, Surface and Coatings Technology. 421 (2021) 127387. https://doi.org/10.1016/j.surfcoat.2021.127387.

[17] R.L. Martins, D.D. Damm, E.J. Corat, V.J. Trava-Airoldi, D.M. Barquete, Mitigating residual stress of high temperature CVD diamond films on vanadium carbide coated steel, Journal of Vacuum Science & Technology A. 39 (2021) 013401. https://doi.org/10.1116/6.0000607.

[18] M. Chandran, A. Hoffman, Diamond film deposition on WC–Co and steel substrates with a CrN interlayer for tribological applications, J. Phys. D: Appl. Phys. 49 (2016) 213002. https://doi.org/10.1088/0022-3727/49/21/213002.

[19] J. Breza, M. Kadlečíková, M. Vojs, M. Michalka, M. Veselý, T. Daniš, Diamond icosahedron on a TiN-coated steel substrate, Microelectronics Journal. 35 (2004) 709–712. https://doi.org/10.1016/j.mejo.2004.06.020.

[20] R.K. Singh, D.R. Gilbert, J. Fitz-Gerald, S. Harkness, D.G. Lee, Engineered Interfaces for Adherent Diamond Coatings on Large Thermal-Expansion Coefficient Mismatched Substrates, Science. 272 (1996) 396–398. https://doi.org/10.1126/science.272.5260.396.

[21] D.D. Damm, A. Contin, F.C. Barbieri, V.J. Trava-Airoldi, D.M. Barquete, E.J. Corat, Interlayers Applied to CVD Diamond Deposition on Steel Substrate: A Review, Coatings. 7 (2017) 141. https://doi.org/10.3390/coatings7090141.

[22] Laser surface texturing to enhance adhesion bond strength of spray coatings – Cold spraying, wire-arc spraying, and atmospheric plasma spraying, Surface and Coatings Technology. 352 (2018) 642–653. https://doi.org/10.1016/j.surfcoat.2017.05.007.

[23] X. Meng, K. Zhang, X. Guo, C. Wang, L. Sun, Preparation of micro-textures on cemented carbide substrate surface by plasma-assisted laser machining to enhance the PVD tool coatings adhesion, Journal of Materials Processing Technology. 288 (2021) 116870. https://doi.org/10.1016/j.jmatprotec.2020.116870.

[24] H. Wako, T. Abe, T. Takagi, T. Ikohagi, Comparison of diamond film adhesion on molybdenum substrates with different surface morphologies, Applied Surface Science. 256 (2009) 1466–1471. https://doi.org/10.1016/j.apsusc.2009.09.004.

[25] M. Amaral, F. Almeida, A.J.S. Fernandes, F.M. Costa, F.J. Oliveira, R.F. Silva, The role of surface activation prior to seeding on CVD diamond adhesion, Surface and Coatings Technology. 204 (2010) 3585–3591. https://doi.org/10.1016/j.surfcoat.2010.04.031.

[26] X. Li, J. Ye, H. Zhang, T. Feng, J. Chen, X. Hu, Sandblasting induced stress release and enhanced adhesion strength of diamond films deposited on austenite stainless steel, Applied Surface Science. 412 (2017) 366–373. https://doi.org/10.1016/j.apsusc.2017.03.214.

[27] R. Börner, M. Penzel, T. Junge, A. Schubert, Design of Deterministic Microstructures as Substrate Pre-Treatment for CVD Diamond Coating, Surfaces. 2 (2019) 497–519. https://doi.org/10.3390/surfaces2030037.

[28] R. Kromer, S. Costil, J. Cormier, D. Courapied, L. Berthe, P. Peyre, M. Boustie, Laser surface patterning to enhance adhesion of plasma sprayed coatings, Surface and Coatings Technology. 278 (2015) 171–182. https://doi.org/10.1016/j.surfcoat.2015.07.022.

[29] Y. Xiao, W. Shi, Z. Han, J. Luo, L. Xu, Residual stress and its effect on failure in a DLC coating on a steel substrate with rough surfaces, Diamond and Related Materials. 66 (2016) 23–35. https://doi.org/10.1016/j.diamond.2016.03.009.

[30] H. Ling, Z.Q. Xie, Y. Gao, T. Gebre, X.K. Shen, Y.F. Lu, Enhanced chemical vapor deposition of diamond by wavelength-matched vibrational excitations of ethylene molecules using tunable CO2 laser irradiation, Journal of Applied Physics. 105 (2009) 064901. https://doi.org/10.1063/1.3082090.

[31] D.M.P. Holland, D.A. Shaw, M.A. Hayes, L.G. Shpinkova, E.E. Rennie, L. Karlsson, P. Baltzer, B. Wannberg, A photoabsorption, photodissociation and photoelectron spectroscopy study of C2H4 and C2D4, Chemical Physics. 219 (1997) 91–116. https://doi.org/10.1016/S0301-0104(97)00090-6.

[32] S.M. Guo, C.C. Lai, T.V. Jones, M.L.G. Oldfield, G.D. Lock, A.J. Rawlinson, Influence of Surface Roughness on Heat Transfer and Effectiveness for a Fully Film Cooled Nozzle Guide Vane Measured by Wide Band Liquid Crystals and Direct Heat Flux Gages, Journal of Turbomachinery. 122 (2000) 709–716. https://doi.org/10.1115/1.1312798.

[33] J. Achard, A. Tallaire, R. Sussmann, F. Silva, A. Gicquel, The control of growth parameters in the synthesis of high-quality single crystalline diamond by CVD, Journal of Crystal Growth. 284 (2005) 396–405. https://doi.org/10.1016/j.jcrysgro.2005.07.046.

[34] H.-G. Jentsch, G. Rosenbauer, S.M. Rosiwal, R.F. Singer, Graphite interlayer formation during CVD diamond coating of iron base alloys: The analogy to metal dusting, Advanced Engineering Materials. 2 (2000) 369–374. https://doi.org/10.1002/1527-2648(200006)2:6<369::AID-ADEM369>3.0.CO;2-8.

[35] P. Lu, K. Chou, R. Schad, XRD Stress Analysis of Nano-diamond Coatings on WC-Co Substrates, 2010.

[36] R. Haubner, M. Rudigier, Raman Characterisation of Diamond Coatings Using Different Laser Wavelengths, Physics Procedia. 46 (2013) 71–78. https://doi.org/10.1016/j.phpro.2013.07.047.

[37] S.R. Sails, D.J. Gardiner, M. Bowden, J. Savage, D. Rodway, Monitoring the quality of diamond films using Raman spectra excited at 514.5 nm and 633 nm, Diamond and Related Materials. 5 (1996) 589–591. https://doi.org/10.1016/0925-9635(96)90031-X.

[38] Q.H. Fan, J. Grácio, E. Pereira, Residual stresses in chemical vapour deposited diamond films, Diamond and Related Materials. 9 (2000) 1739–1743. https://doi.org/10.1016/S0925-9635(00)00284-3.

[39] J.W. Ager, M.D. Drory, Quantitative measurement of residual biaxial stress by Raman spectroscopy in diamond grown on a Ti alloy by chemical vapor deposition, Phys. Rev. B. 48 (1993) 2601–2607. https://doi.org/10.1103/PhysRevB.48.2601.

[40] J.S. Kim, M.A. Cappelli, A model of diamond growth in low pressure premixed flames, Journal of Applied Physics. 72 (1992) 5461–5466. https://doi.org/10.1063/1.351989.

CRediT authorship contribution statement

Zhipeng Wu: Methodology, Data curation, Formal analysis, Investigation, Writing-original draft, Writing-review & editing. **Wanting Sun**: Formal analysis, Investigation, Writing-review & editing. **Qiuchi Zhu**: Methodology, Formal analysis. **Xin Chen**: Formal analysis. **Xiang Zhang**: Formal analysis. **Lanh Trinh**: Formal analysis. **Nan Li**: Software. **Aofei Mao**: Writing-review & editing. **Xi Huang**: Writing-review & editing. **Nada Kraiem**: Writing-review & editing. **Jean-François Silvain**: Conceptualization. **Bai Cui**: Resources, Project administration, Funding acquisition. **Yongfeng Lu**: Resources, Conceptualization, Project administration, Funding acquisition.

Zhipeng Wu and **Wanting Sun** contributed equally.

Graphical abstract

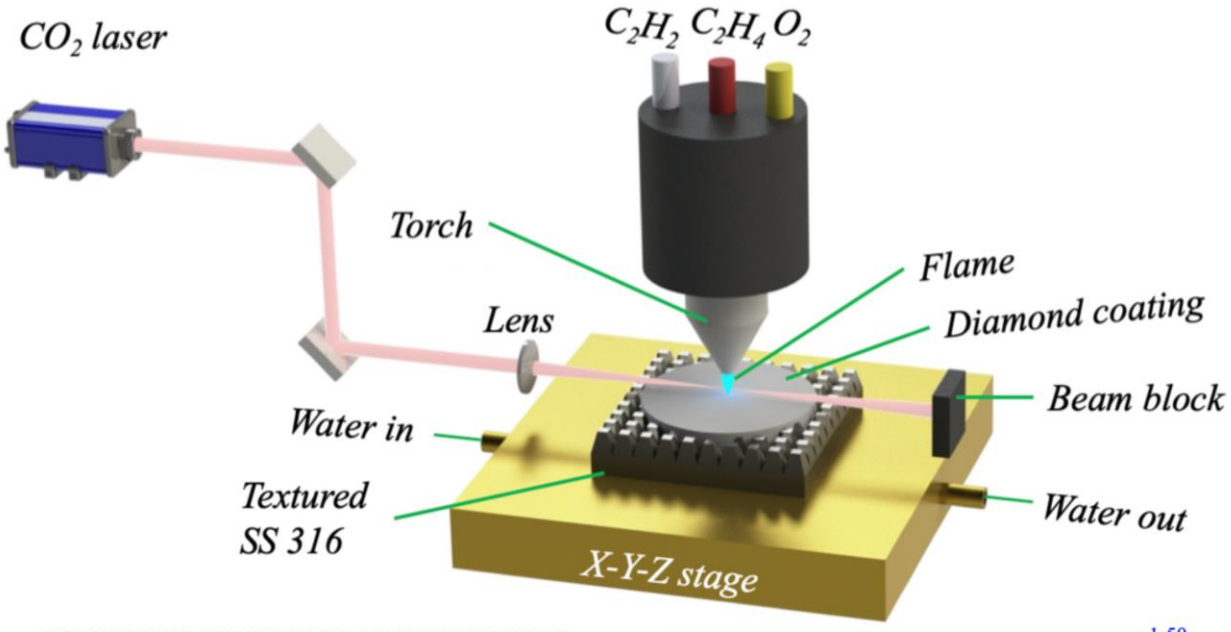

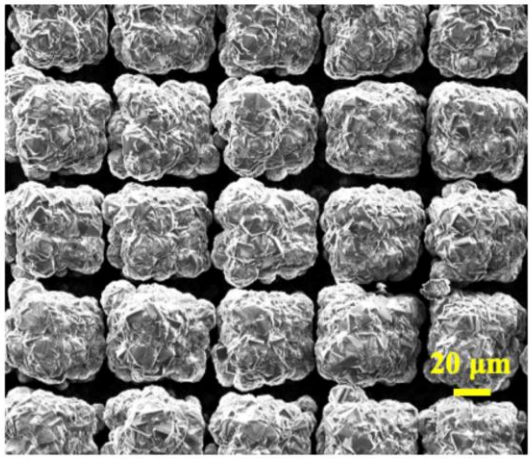

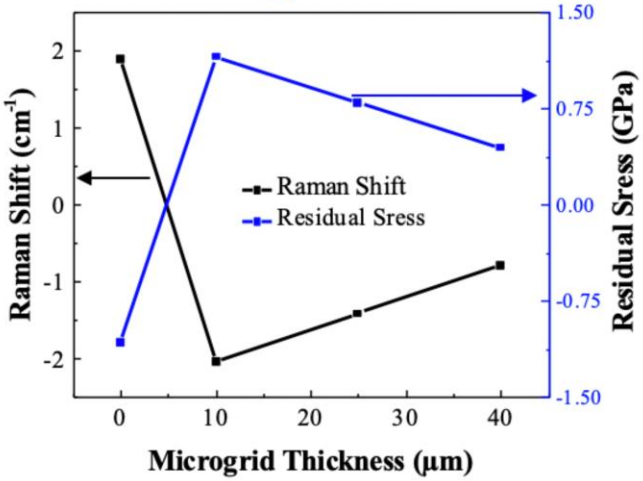

Highlights:

- The diamond coatings on the femtosecond-laser-textured SS 316 substrates exhibited superior adherence compared to those deposited on the SS 316 substrate with a smooth surface. This enhanced performance is attributed to stress relief and improved mechanical bonding resulting from the laser texturing.

- The diamond coatings on the femtosecond-laser-textured SS 316 substrates demonstrated accelerated growth speed and improved quality as the microgrid depth, generated through fs-laser texturing, increased.

- A diamond coating with a maximum thickness of 19 μm and a quality factor of up to 96% can be obtained on femtosecond laser-textured SS 316 substrates.

- The growth kinetics of diamond coatings on these substrates were systematically investigated.